

See discussions, stats, and author profiles for this publication at: <https://www.researchgate.net/publication/341134464>

Adversarial gesture generation with realistic gesture phasing

Preprint · April 2020

CITATIONS

0

READS

133

3 authors, including:



Ylva Ferstl

Trinity College Dublin

14 PUBLICATIONS 75 CITATIONS

[SEE PROFILE](#)

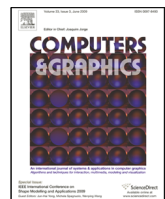


Rachel McDonnell

Trinity College Dublin

92 PUBLICATIONS 1,273 CITATIONS

[SEE PROFILE](#)



Adversarial gesture generation with realistic gesture phasing

Ylva Ferstl^a, Michael Neff^b, Rachel McDonnell^a

^aTrinity College Dublin

^bUniversity of California Davis

ARTICLE INFO

Article history:

Received May 4, 2020

Keywords: gesture generation, machine learning, generative adversarial networks, gesture segmentation, virtual humans

ABSTRACT

Conversational virtual agents are increasingly common and popular, but modeling their non-verbal behavior is a complex problem that remains unsolved. Gesture is a key component of speech-accompanying behavior but is difficult to model due to its non-deterministic and variable nature. We explore the use of a generative adversarial training paradigm to map speech to 3D gesture motion. We define the gesture generation problem as a series of smaller sub-problems, including plausible gesture dynamics, realistic joint configurations, and diverse and smooth motion. Each sub-problem is monitored by separate adversaries. For the problem of enforcing realistic gesture dynamics in our output, we train three classifiers with different levels of detail to automatically detect gesture phases. We hand-annotate and evaluate over 3.8 hours of gesture data for this purpose, including samples of a second speaker for comparing and validating our results. We find adversarial training to be superior to the use of a standard regression loss and discuss the benefit of each of our training objectives. We recorded a dataset of over 6 hours of natural, unrehearsed speech with high-quality motion capture, as well as audio and video recording.

© 2020 Elsevier B.V. All rights reserved.

1. Introduction

Interactive virtual agents are becoming increasingly common and people may enjoy interacting with them more than ever with realistic video-based characters [1]. However, they often still feel stiff and unnatural. Non-verbal behavior plays an important role in making these agents more appealing, and co-speech gestures specifically are a key component for increasing user engagement [2]. Automatic generation of such gesturing behavior for given utterances is appealing due to both cost

factors and time constrained animation needs. Despite much research in the area, automatically generating realistic gestural behavior remains an open problem. One of the difficulties in modelling the speech-to-gesture relation is the asynchronicity between the two channels; gesture precedes or co-incides with speech but rarely follows [3], making real-time prediction nearly impossible. A second difficulty is the highly non-deterministic mapping of speech to motion. Even the same speaker uttering the same phrase will likely perform different gesture motions on each repetition. Gestures may also communicate information not provided explicitly through speech, providing complementary, not redundant information [4, 5].

e-mail: yferstl@tcd.ie (Ylva Ferstl), mpneff@ucdavis.edu (Michael Neff), ramcdonn@scss.tcd.ie (Rachel McDonnell)

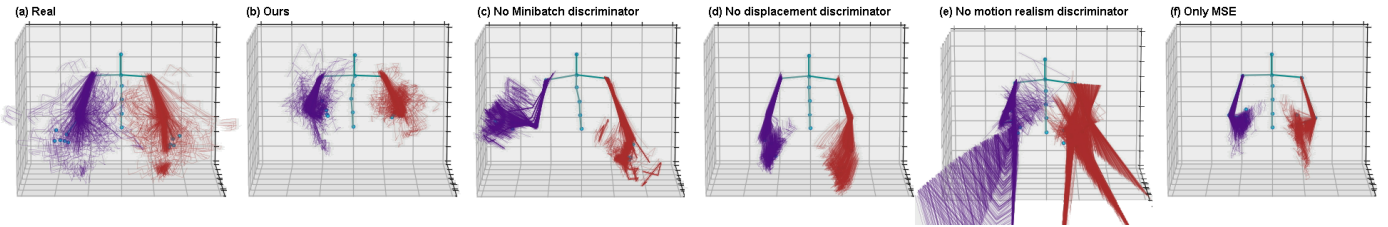


Fig. 1. Motion distribution over 2 minutes, plotted at 4 fps. For one example clip, a) shows the real data distribution, b) the distribution with our method, c-e) examples of excluding specific training objectives, and f) the distribution for a model trained with a standard regression loss.

1 The non-deterministic mapping of speech to motion means
 2 for one utterance, multiple variations of a gesture (or no ges-
 3 ture at all) may be perceived as plausible by an observer. This
 4 presents a difficulty in training a speech-to-gesture model; even
 5 a plausible produced gesture may be penalized when it is nu-
 6 merically far from the exact gesture found in the dataset for this
 7 utterance. A standard regression loss in training a speech-to-
 8 gesture model is therefore not ideal.

9 In this work, we apply two novel techniques for training a re-
 10 current neural network (RNN) producing gesture motion based
 11 on input speech. Firstly, we train a speech-input-motion-output
 12 RNN with a generative adversarial paradigm instead of a stan-
 13 dard regression loss, and we specifically use multiple adver-
 14 saries instead of a single one.

15 Secondly, we study the phase structure of a gesture dataset
 16 and train a classifier to automatically detect these phases. The
 17 phase structure of natural gesture describes the dynamics and
 18 functions of motion segments within it, and can be divided into
 19 distinct parts: preparation, stroke, holds, and retraction. The
 20 expression of these phases and their sequencing may vary from
 21 speaker to speaker, making their labelling a difficult and at times
 22 ambiguous task.

23 In this work, we extend Ferstl et al. [6], with additional con-
 24 tent regarding gesture phasing, including new results on our au-
 25 tomatic phase classification, with a more speaker-flexible re-
 26 duced phase model focusing on the stroke phase, the essential
 27 core of a gesture. We furthermore annotate gesture samples of
 28 a second speaker exhibiting a distinctly different gesture style
 29 in order to evaluate our automatic phase classification.

30 In an adversarial training paradigm, we use the automatic
 31 phase labelling to extract the phase structure of real and gen-

erated motion. Producing realistic phase structures becomes a
 32 training objective of the generator, enforced by a discriminator
 33 specifically designed for distinguishing phase sequences.

34 The set of training objectives further includes humanoid
 35 skeleton constraints, and utterance match and diversification
 36 objectives, each represented by separate discriminators.

37 Our multi-discriminator design allows the gesture generation
 38 problem to be defined with multiple smaller sub-problems. We
 39 discuss how each of our discriminator objectives improves the
 40 final result.

41 We will first introduce the phase classifier in Section 4, be-
 42 fore discussing the speech-to-gesture model in Section 5 and its
 43 adversarial training in Section 7.

2. Related work

2.1. Gesture generation

44 Various methods have been proposed for generating gesture
 45 from speech. Some approaches employ rule-based systems that
 46 rely on explicitly defined text-to-gesture rules [7, 8, 9]. Other
 47 works have used statistical modelling estimating conditional
 48 probabilities for speech features co-occurring with motion fea-
 49 tures [10, 11, 12]. Many animation systems have been devel-
 50 oped to produce gesture motion, such as SmartBody [13, 14];
 51 while it is beyond the scope of this work to cover this area in
 52 detail, recent surveys provide an overview (e.g. [15]).

53 Machine learning approaches have both been used in a fully
 54 automatic manner without any need for hand annotating data
 55 [16, 17, 18, 19, 20], as well as in conjunction with hand-
 56 labelled, higher-level features such as gestural signs [21].

57 Recent work has explored recurrent networks for speech-
 58 to-gesture generation for English [22] and Japanese speech

[23, 24]. Such a network uses recurrent connections between network activations at consecutive time-steps to model data with temporal dependencies. Recurrent networks can, for example, capture the dynamics of a motion pattern well and have been successfully employed for human motion modelling tasks [25, 26]. However, recurrent networks trained with a standard error function tend to suffer from mean pose convergence, where longer term motion sequences quickly regress to the average pose (such as in Martinez et al. [27] and Jain et al. [28]). This may be due to error accumulation when feeding generated output back into the network [29], resulting in damped motion that may look constrained and unrealistic. Generative adversarial networks (GANs) have been proposed as one alternative training paradigm. Here, instead of minimizing a standard error function such as the mean squared error (MSE) of joint positions or angles, the model’s objective is to produce output that is qualitatively similar to real data, as judged by another model, the discriminator, that is trained simultaneously in conjunction with the generator. GANs have been successful in human motion modelling tasks [30, 31], as well as in a head motion from speech generation task [32].

Recent work proposed a convolutional network combining a standard L1 regression loss with an adversarial discriminator for predicting 2D gesture motion from speech [33]. The authors represent audio visually as a spectrogram, which is then encoded by an audio encoder and subsequently processed by a UNet translation architecture [34]. The authors created a large dataset of over 140 hours of 2D pose keypoints extracted from YouTube videos of 10 speakers. (This work and dataset was not yet available at the time of our work). The speakers are professional performers, such as John Oliver (*Last Week Tonight*) and Seth Meyers (*Late Night with Seth Meyers*), producing largely rehearsed speech and generally producing a relatively small set of clear gesture motions. Their speaker-specific models generate sequences rated equally good as mismatched real gesture samples, as measured by the rate it fooled human participants. The failure to surpass random real motion is an indication of the difficulty of the speech-to-gesture task. In our work, we focus

on a different type of gesture motion, namely spontaneous, conversational speech gestures that appear more diverse and qualitatively different from the distinct gestures usually seen for professional performers (refer e.g. to John Oliver’s performances in *Last Week Tonight*). 39
40
41
42
43

2.2. Gesture phase

Natural gesture behavior consists of phases with qualitatively different dynamic characteristics [35] and these phases occur in specific patterns [36]. In the *preparation* phase, the hands are moved into position for the gesture. The *stroke* is the expressive phase of a gesture and has the most focused energy; it is an “accented movement” with Effort in the sense of Laban [36], conveying a sense of intention and meaning of the motion. It is the main meaning-carrying movement of the gesture, often describing a specific shape that relates to the accompanying verbal phrase [3]. The *retraction* moves the limbs back into a restful position (an incomplete retraction is noted as a *partial retraction*). *Holds* are segments with zero velocity and may occur before or after the stroke [37]. All phases are optional except the stroke. 44
45
46
47
48
49
50
51
52
53
54
55
56
57
58
59
60
61
62
63
64
65
66
67
68
69
70
71
72
73
74
75
76

We aim to capture these specific dynamic phases in our gesture generation system. While these phases are present in any natural gesture data, capturing the phase structure implicitly would arguably require a large dataset. Instead, we explicitly segment the phase structure of gesture motion.

Segmenting gesture motion into its phases is non-trivial and in many cases requires subjective judgment. Hence the labelling process cannot be seen as deterministic and 100% accuracy is unlikely, or even impossible. Often, gesture phases can be straightforward to identify, but in other cases, it may be more difficult. This tends to occur when one stroke goes directly into another or if a stroke starts from a retract position. Consider for example the ambiguous example of a gesture sequence in Figure 2, where both step (1) and (3) are considered a stroke phase: One could consider the motion to the middle transition frame (2) either a partial-retract of the first stroke in (1) or a preparation for the second stroke in (3).

Different, automatic gesture phase annotation methods have

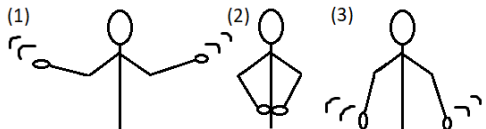


Fig. 2. Ambiguity in gesture sequence labelling. If steps (1) and (3) are each considered a gesture stroke, the motion to the transition step (2) may be labelled as either a partial-retract of the preceding stroke or a preparation phase for the following stroke.

been proposed, including the use of support vector machines [38] and hidden Markov models [39, 40]. One limiting factor in training phase models is obtaining labelled data; segmenting just one minute of video into gesture phases may take one hour or more of work (e.g. [10]). Previous work has therefore often focused on simpler sub-problems of detecting whether one specific phase is occurring (e.g. detection only of gesture strokes), or whether a gesture is being performed at all [40, 41, 42].

Another difficulty in automatic phase detection is the difference in phase structure as well as phase expression between speakers and even within speaker. Phase structure differences can include overall gesture rate as well as differences in the distribution of phases; for example, one speaker may regularly produce two or more gesture strokes before returning to a rest position, while another speaker may average just one stroke before returning to rest [43]. Phase expression such as the stroke velocity profile can vary not only from speaker to speaker, but also between recordings of the same speaker [38]. This variability makes the task of automatic classification challenging, and, for a new, unseen speaker, particularly error-prone. Nevertheless, we consider even imperfect phase labelling a useful and reasonable way to explicitly describe different motion profiles present within a gesture, separating effortful, accented gesture strokes from less accented preparation and retraction as well as still hold phases. In this work, we focus on modelling just one speaker and his gesture dynamics to maximise training consistency of gesture dynamics in the training set.

3. Dataset

We recorded a high-quality dataset of natural speech and 3D motion specifically for the purpose of this work. We used a single male actor for the complete recording. The actor is a

native English speaker producing spontaneous conversational speech without interruptions, i.e., without verbal cues from a conversation partner. The actor was free to choose any topic in his speech but mostly covered personal stories and sports. We chose an actor with naturally frequent gesturing behavior, but he was unaware of the purpose of the recording. The actor addressed a person situated behind the camera in order to give him the visual feedback of a conversation partner. We recorded 25 takes, ranging between 10 and 20 minutes each, totalling over 370 minutes (more than 6 hours) of data. The actor's motion was captured with a 59 marker setup and 20 Vicon cameras at 120 fps (frames per second). Audio was recorded at 44 kHz. Video was captured with two cameras, one capturing a full body shot and the second camera capturing a higher-quality close-up shot of the face and parts of the upper body.

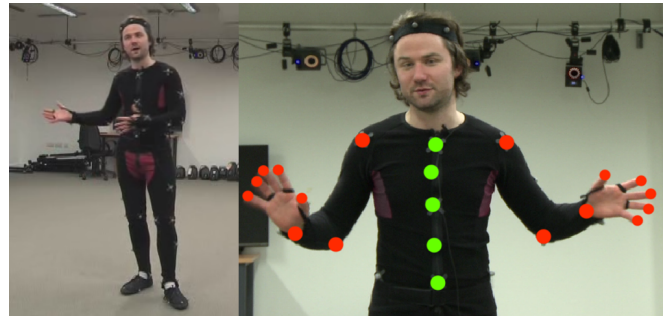


Fig. 3. Capture setup and location of joints. The 16 red markings indicate the joints used for the gesture phase classification. The five green markings indicate the spinal joints added to the joint set for gesture motion prediction.

3.1. Data pre-processing

We process the recorded speech with openSMILE [44] to extract 26 Mel Frequency Cepstral Coefficients (MFCCs), as well as the F0 (pitch) value. MFCCs are commonly used in speech recognition tasks and the F0 value as a prosodic feature carries information about emphasis. Speech features are extracted with a window size of 20 ms at steps of 10 ms, resulting in data of 100 fps.

We down-sample the motion capture data from 120 to 100 fps to match the speech features. We center and lock the root node of the motion clips to the origin position with zero rotation and then extract the absolute positional values of the captured joints. Our actor remains fairly static in his lower body and

1 we are therefore able to capture most of his dynamics from the
 2 joints upward of the locked root.

3 We normalize all speech and joint position features to zero
 4 mean and unit variance. We train all models on 20 fps; in order
 5 not to lose data, we take 20 fps data from 5 subsequent starting
 6 positions, resulting in 5 sets of 20 fps data.

7 3.2. Gesture phase annotation

8 We annotated the phase structure of a subset of 226 minutes
 9 of the complete dataset using the ANVIL annotation tool [45].
 10 The 226 minutes were selected at random from the dataset. We
 11 aimed to annotate as much of our dataset as possible while en-
 12 suring annotation quality. For this purpose, we trained six an-
 13 notators whose work was then repeatedly cross-checked at the
 14 start, before each annotator was assigned separate data clips.
 15 We annotated nine different gesture phases; (1) preparation, (2)
 16 stroke, (3) pre-hold, (4) hold, (5) independent hold, (6) rest
 17 hold, (7) partial retract, (8) retract, and (9) ‘none’. Table 1
 18 shows the frequency of each phase within the annotated data
 19 subset. *Pre-hold* and *hold* occur before and after the gesture,
 20 respectively. *Independent hold* occurs when a gesture has no
 21 stroke, but is defined by a held pose. *Rest hold* occurs when the
 22 hands are held in a relaxed position after a partial retract, with-
 23 out being fully retracted to the sides of the body. *None* occurs
 24 when no gesture is being performed; the arms are either fully
 25 retracted to the sides of the body or a no-gesture movement such
 26 as a self-adaptor is occurring.

27 Our speaker performs on average 38.1 gesture strokes per
 28 minute, or one gesture every 1.6 seconds. Assuming roughly
 29 the same gesture frequency in the remaining un-annotated 140
 30 minutes of data, we estimate that our dataset contains approxi-
 31 mately 14,000 gestures.

32 We computed pairwise coder agreement with ANVIL [45]
 33 by double-annotating five samples totalling 50 minutes of
 34 data, each with a different annotator combination. We found
 35 high segmentation agreement, averaging 98.5% ($\min=95.5\%$,
 36 $\max=99.9\%$), indicating high consistency in detecting phase
 37 boundaries. For the overall coding agreement that includes
 38 segment (or phase) labels, we achieved moderate agreement

39 as defined by Krippendorff’s alpha value [46], with a mean of
 40 $\bar{\alpha} = 0.46$ ($\alpha_{min} = 0.39$, $\alpha_{max} = 0.5$). As we pool all hold cat-
 41 egories for the phase classifier in Section 4, we compare Krip-
 42 pendorff’s alpha value for the case of treating post-stroke holds,
 43 pre-holds, rest-holds and independent holds all as a uniform
 44 hold category: $\bar{\alpha} = 0.47$, $\alpha_{min} = 0.43$, $\alpha_{max} = 0.53$.

45 In order to evaluate the robustness of our automatic phase
 46 classification in Section 4, we annotated a short sample of ges-
 47 turing of a second speaker. For this, we took samples of just un-
 48 der 5 minutes of data from the Trinity Speech-Gesture dataset
 49 [22]. This sample was not included in the training set and only
 50 used for evaluation. The speaker in the Trinity Speech-Gesture
 51 dataset exhibits a qualitatively very different gesturing style to
 52 that of the speaker in this work, visualized in the supplemen-
 53 tal video. This speaker often incorporates the whole body in a
 54 gesture and rarely stands still. This means that extracting the
 55 motion of the upper body joints does not fully describe the per-
 56 formed gesture, some information will be lost. Hold phases
 57 mark another observable difference between our speaker and
 58 the Trinity Speech-Gesture dataset; whereas holds tend to be
 59 associated with minimal movement in our speaker, the Trinity
 60 Speech-Gesture speaker’s holds appear overall less still, with
 61 the speaker in seemingly constant motion.

62 Our annotated sample of the Trinity Speech-Gesture dataset
 63 suggest a similar gesture stroke frequency as in our database;
 64 we calculate 33.6 gesture strokes per minute. We annotated
 65 160 strokes in this sample. All annotated phase frequencies are
 66 reported and compared to our speaker in Table 1.

67 An example of an annotated gesture sequence is given in Fig-
 68 ure 4.

69 4. Phase classifier

70 Modelling gesture motion from speech directly is a hard
 71 problem. As described in Section 1, the same phrase may
 72 be plausibly accompanied by many different gesture shapes.
 73 Speech features may be more easily associated with the dy-
 74 namics of gesture motion; the kinematics of gestures (e.g.,
 75 speed and acceleration) have been shown to correlate with the

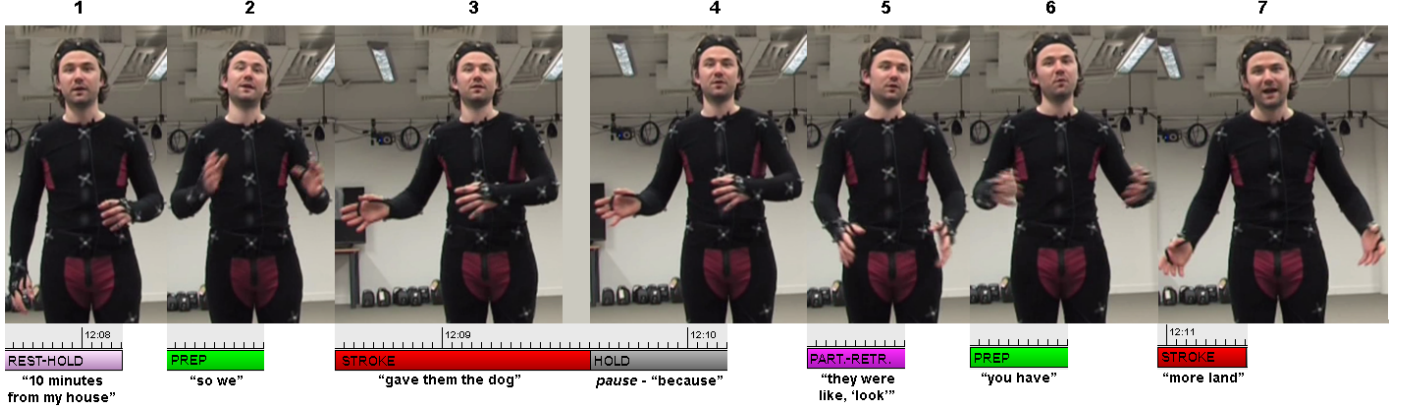


Fig. 4. Sample of an annotated gesture sequence. For each annotated gesture phase, the speaker’s accompanying phrase is given. (1) The hands start in a resting position. (2) The preparation phase brings the hands into position for the gesture. (3) The stroke phase carries the meaning of the gesture (the act of giving). (4) The hands stay in position, the speaker pauses for a moment. (5) The hands are retracted partially towards a restful position. (6) A new preparation phase immediately initializes the next gesture. (7) Another gesture stroke is performed, describing “more”.

Table 1. Frequency of the 9 annotated phases in the total annotation set of 226 minutes.

Gesture phase	Number of occurrences		Percent of annotated time	
	Our speaker	TSG speaker	Our speaker	TSG speaker
Preparation	5775	130	19.1%	14.9%
Pre-hold	979	17	3.2%	1.6%
Stroke	8655	160	39.6%	28.5%
Hold	5100	110	24.8%	26.1%
Independent hold	94	3	0.8%	0.7 %
Rest hold	474	27	3.1%	10.3%
Partial retract	1077	48	3.8%	6.5%
Retract	409	13	1.3%	2.1%
‘None’	475	14	4.2%	9.3%
Total	23038	522	100%	100%

1 prosodic features of speech [47]. However, implicitly inferring
 2 gesture dynamics from raw positional data may be difficult and
 3 require a large amount of data. We therefore model these
 4 dynamics explicitly. Namely, we extract gesture phases as higher-
 5 level representation of the characteristic dynamics of gesture
 6 motion. This representation is sufficiently low-dimensional
 7 (small set of different labels) to model its structure from a rela-
 8 tively small dataset. We hand-annotated the phase structure of
 9 3.75 hours of data (as described in Section 3.2) and trained a
 10 classifier to detect gesture phases of a motion sequence. Our
 11 objective is to use this phase classification to enforce a realistic
 12 phase structure in the gesture generator’s output. A classifier
 13 is necessary so that any new (un-annotated) motion can be seg-
 14 mented into phases and judged for its structural realism. After
 15 training the classifier on the annotated data subset, we never

16 use the true hand-annotated phase labels, we always use the
 17 phase labels determined by the classifier and the full dataset.
 18 An overview of the phase classifier’s role in the final architec-
 19 ture is shown in Figure 5, and will be discussed in more detail
 20 in Section 7.1.

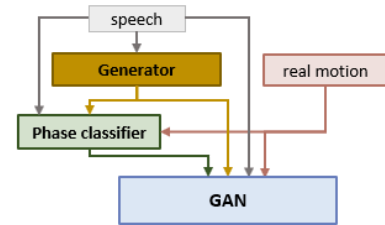


Fig. 5. Overview of the system architecture. The generator receives speech features and produces gesture motion. The multi-discriminator GAN receives three different types of input: (1) the speech features belonging to a motion segment, (2) a motion segment (real or generated), and (3) the phase structure of the motion segment (determined by the phase classifier).

We furthermore train a robust 1-phase classifier for gesture

16
 17
 18
 19
 20

21

1 stroke detection as a useful tool for future gesture analysis. The
 2 stroke phase represents the core, meaning-carrying part of a
 3 gesture, and hence its segmentation is essential for gesture form
 4 analysis.

5 We validate all phase classification models on a second
 6 speaker with different gesture style.

7 *4.1. Method*

8 The classifier assigns one phase label to each time-step of an
 9 input sequence. For training the classifier, we reduce the anno-
 10 tated gesture phase label set from nine to six classes that capture
 11 the main phase types by combining all types of holds into one
 12 class. This reduces the problem of unbalanced class frequen-
 13 cies (e.g. only 94 independent holds out of 23,038 phases), as
 14 well as removing some redundant information (e.g. a hold oc-
 15 curring between preparation and stroke can be assumed to be
 16 a pre-hold; a hold after a partial-retract is a rest-hold). Hence,
 17 we combine the labels ‘pre-hold’, ‘hold’, ‘independent hold’
 18 and ‘rest hold’ into a super-class ‘hold’. In effect, this simpli-
 19 fies the classification task by labelling all still frame sequences
 20 (sections with close-to-zero joint velocities) as one class, with
 21 the exception of the completely retracted ‘none’ position where
 22 the arms are relaxed by the side of the body. As discussed later,
 23 the partial-retract phase proved difficult to classify, so for train-
 24 ing our generative network, we decided to combine it with the
 25 retract class, and due to its rarity we furthermore combine the
 26 fully retracted ‘none’ class into the retract group. For our ad-
 27 versarial training we therefore have four phase classes: Prepa-
 28 ration, holds (including pre-holds, independent holds, and rest-
 29 holds), strokes, and ‘other’. The ‘other’ class combines retracts,
 30 partial retracts, and ‘none’ annotations. We believe this sub-
 31 set captures the most essential dynamics of gesture motion; we
 32 consider holds and strokes the most important representatives of
 33 gesture dynamics and their separation tends to get lost in stan-
 34 dard training of recurrent networks (mean pose convergence
 35 leading to smoothed, damped motion). Second, we separate
 36 the preparation phase due to its high frequency and relevance
 37 in the gesture structure. Retracts are relatively infrequent for
 38 our speaker, as is the ‘none’ phase (completely retracted po-

39 sition); we decided to pool these classes together to make for
 40 a higher confidence model and a more achievable task for the
 41 gesture generator. The phase labels produced by the classifier
 42 are used as pseudo ground-truth during adversarial training, and
 43 we therefore need the classifier to be as confident as possible in
 44 its decisions.

45 *4.2. Network architecture and training*

46 The classifier processes sequences of 100 time steps (5 sec-
 47 onds at 20 fps), and assigns a phase label to each step. The
 48 input of the classifier are the x, y and z directional velocities
 49 of 16 joints (total of 48 values), corresponding to the shoulder,
 50 elbow, wrist, and each fingertip, as well as the corresponding
 51 pitch value. The pitch value captures information about speech
 52 emphasis and using a single speech feature ensures we are not
 53 increasing the input space significantly and hence minimize the
 54 network’s ability to overfit. Including pitch improves our classi-
 55 fication scores (see Table 2), in line with the finding that speech
 56 is associated with gesture phase [48].

57 The network is visualized in more detail in Figure 6, but gen-
 58 erally consists of a two-layer recurrent network with an addi-
 59 tional densely connected NN (neural network) layer for input
 60 processing. The recurrent layers are Long Short Term Memory
 61 (LSTM) cells; specifically, a unidirectional LSTM in the first
 62 recurrent layer, and a bidirectional LSTM in the second recur-
 63 rent layer. LSTM cells can handle sequential data, such as time
 64 series data, and bidirectional LSTMs specifically take both past
 65 and future data into account for predicting a time step. We reg-
 66 ularize the network by applying dropout after each layer and
 67 batch normalization before the final output. Dropout rates are
 68 empirically determined to provide good performance without
 69 overfitting.

70 Of our total of 226 minutes of annotated data, we separate
 71 6.5 minutes of validation data by randomly selecting 13 start
 72 indices from which to take 30 seconds of data without over-
 73 lap. Composing the validation data of snippets from multiple
 74 takes this way ensures that the validation performance is not
 75 annotator- or take-specific. The remaining annotations serve as
 76 training data.

1 We trained three classification models for segmenting ges-
 2 ture. Firstly, we train a 6-class model distinguishing all an-
 3 notated phases (pooling all hold categories), second, a 4-class
 4 classifier pooling rare phases into an ‘other’ class, and third, a
 5 1-class model for detecting only the core stroke phase with in-
 6 creased confidence. For the two multi-phase models, we train a
 7 version each with and without speech pitch input; the network
 8 details are visualized in Figure 6. For the stroke classifier, we
 9 predict a single class, the stroke phase, which is the essential
 10 phase in gesture. This allows for more confident classification
 11 when dealing with different speaker styles, extending the ap-
 12 plicability of this work. The stroke classifier is visualized in
 13 Figure 7. The output layer applies a softmax activation in the
 14 case of the 4- and 6-class model, and a sigmoid activation in
 15 the single-class stroke classifier. The differences in network
 16 architecture between the 3 classifiers results from empirically
 17 finding the best performing configuration for each number of
 18 classes. The number and size of recurrent layers was chosen
 19 based on the best found trade-off between modelling capacity
 20 and generalizability, i.e. reaching good performance without
 21 overfitting.

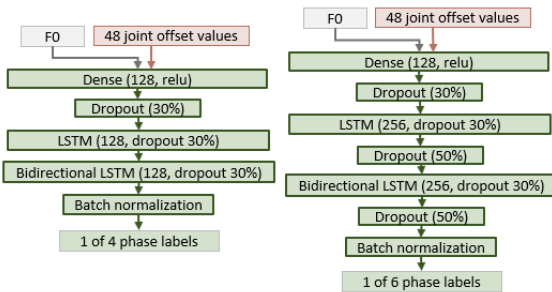


Fig. 6. The two detailed network configurations for our 4-phase classifier and our 6-phase classifier. ‘Dense’ denotes a standard densely connected NN layer. In brackets are denoted the layer size or the dropout ratio. The 48 joint values refer to the x, y, and z offsets of the 16 joints shown in Figure 3.

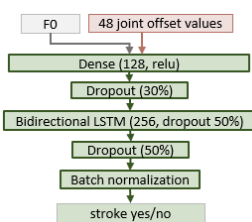


Fig. 7. The network configurations for our 1-phase (stroke) classifier.

4.3. Results

4.3.1. Multi-phase classifiers

The multi-phase classifiers reach an overall weighted F-score of 0.76 for both the 4-class and the 6-class model. The detailed results can be seen in Table 2. The stroke and hold phases reach the highest scores; this is likely due to both their distinct dynamics as well as their high frequency in the training set (see Table 1). Lower frequency phases with less distinct dynamics, such as partial retracts, are more difficult to detect. Furthermore, partial-retracts and preparation phases both average a length of less than 500 ms, making them potentially harder to catch as well as align; at our training sample rate of 20 fps, a prediction with just one frame of erroneous shift would only yield an 80% score. Notably, the annotated phase labels are only pseudo ground truth, as determined by an annotator, resulting in some inconsistencies and errors. Inter-rater category agreement for our evaluation samples averages 64.4%, capping the realistically achievable score for the phase classifier.

Since the input is always a sequence of 5 seconds from a randomly drawn starting point, the classifier has limited context information for predicting the phase label of a time step. Providing the label of the phase preceding a sequence or increasing sequence length may improve classification results.

Validating our classifiers on the annotated sample of the Trinity Speech-Gesture dataset (denoted as ‘TSG speaker’), the 4-class model proves more robust with an F-score of 0.69. The 6-class model reaches a score of 0.65, with the weakness lying in the less common classes, particularly partial-retract. The most confidently predicted class throughout all model versions and across both speakers is the ‘hold’ class; this may be the easiest class to extract as it contains almost all sections of zero velocity. Possible exceptions are the no-gesture sections annotated as ‘none’, though our speaker tends to swing his arms during these and indeed not stay still.

We compare results for the two multi-phase classification models (4-class and 6-class), with and without speech pitch input (Table 2). The benefit of including pitch in the input to the classifier is more pronounced for the 6-class model, where all individual scores except ‘partial retract’ are improved by in-

cluding pitch, as well as showing an improvement of 0.03 in the overall weighted F-score. For the 4-class model, the individual class scores improve (all except stroke) or remain the same (stroke), but the weighted overall F remains the same when including pitch as input. We also report the performance of the no-pitch models on the second speaker. No benefit is apparent for including pitch of the second speaker; this may be due to the articulation differences between the training and the validation speaker and using the pitch derivative instead could address this.

We compare our results with the work of Madeo et al. [38] (Figure 2), who employ a hierarchical strategy of single-class classifiers, where e.g. a hold classifier first detects all holds, subsequently a stroke classifier detects all strokes in the remaining data, etc. Their results represent the best scores across multiple models rather than a single model encompassing all gesture classes. That is, they trained combinations of single-class classifiers and the here reported results represent the highest scores for each class across combinations. For example, the model achieving the score of 0.79 for detecting a preparation phase is not the same model that achieves the score of 0.79 for stroke detection. Another significant difference to our work lies in the dataset composition; Madeo et al. [38] restrict the two captured participants to describing one of three comic strips. Their results indicate high dependence of performance on the comic story the classifiers were trained on (significantly reduced performance when training and test data were taken from different comic strip retellings), as well as on which participant a classifier was trained on. As our dataset was captured across multiple days, with a large variety of spontaneous, uncued gestures, the performance of the classifiers presented in Madeo et al. [38] would likely not be adequate for this work.

4.3.2. Stroke classifier

The stroke classifier reaches a weighted average F-score of 0.83 on the speaker it has been trained on (our speaker), and a score of 0.82 on the validation speaker. Inter-coder category agreement for the case of stroke/ no stroke is naturally higher than for the full set of gesture phases, averaging 74.3%. In-

terestingly, it can be seen that the stroke classification score (first line in Table 3) is the same as in the 4-class model, reaching 0.79 for the training set speaker, and 0.72 for the validation speaker (the 6-class model coming very close with 0.78 and 0.71, respectively), suggesting that we may be reaching the maximum score possible with an imperfect training set. The higher phase label consistency of the stroke training set may therefore be the main reason for the more robust classification.

4.4. Discussion

Looking at the relationship between the achieved F-scores and the inter-rater category agreement, we hypothesize that improving coder agreement would much improve classification results. We believe future improvements on the phase classification should focus on improving the training data consistency rather than the classification model.

The robust classification score of the stroke classifier for both our speaker as well as the validation speaker makes it a good tool for future gesture analysis. As the stroke phase represents the essential, meaning-carrying part of a gesture, stroke segmentation is useful for additional information extraction such as gesture form detection.

It is less straightforward to train a classifier for other single phase types, as was done with the stroke present/ not present classifier. Since other phases occur less often across the training set, splitting our dataset into e.g. preparation/ no preparation would result in about a 1:5 ratio. Such unbalanced classifiers are more difficult to train, requiring a weighted loss function or an adapted (balanced) dataset (the latter resulting in a smaller training dataset).

‘Hold’ predictions may be more easily segmented by simply computing sections of close to zero velocity, and this could aid additional segmentation by an annotator as well as increase inter-coder consistency.

5. Gesture generator

The gesture generator is the core of our system and models the speech-to-gesture translation. The generator receives

Table 2. F-scores of phase classifier. Results without pitch input are reported in brackets behind the results with pitch input. Our ‘other’ class combines the labels *retract*, *partial retract*, and *none*. The results denoted as TSG correspond to our validation speaker taken from the Trinity Speech-Gesture dataset.

Gesture phase	4 classes	4 classes	6 classes	6 classes	F-score
		TSG speaker		TSG speaker	Madeo et al. [38]
Preparation	0.64 (0.63)	0.56 (0.55)	0.65 (0.64)	0.56 (0.51)	0.79
Stroke	0.79 (0.79)	0.72 (0.7)	0.79 (0.78)	0.71 (0.71)	0.79
Hold	0.83 (0.82)	0.76 (0.76)	0.81 (0.78)	0.74 (0.77)	0.58
Partial retract	-	-	0.47 (0.49)	0.39 (0.35)	-
Retract	-	-	0.73 (0.70)	0.54 (0.52)	0.5
‘None’	-	-	0.75 (0.56)	0.51 (0.59)	-
‘Other’	0.64 (0.6)	0.58 (0.54)	-	-	-
Overall	0.76 (0.76)	0.69 (0.67)	0.76 (0.73)	0.65 (0.66)	

Table 3. F-scores of the stroke classifier.

Gesture phase	Our speaker	TSG speaker
Stroke	0.79	0.72
No stroke	0.85	0.86
Overall	0.83	0.82

1 speech features as input and produces the positions of the 21
2 joints shown in Figure 3.

3.1. Generator architecture

4 The generator receives 27 speech features as input, composed
5 of 26 MFCC values and the speech pitch (F0) value. The gen-
6 erator then infers the x, y, and z positions of 21 joints: the hand,
7 arm, and spine joints depicted in Figure 3.

8 The generator architecture is visualized in Figure 8. The
9 speech input is processed by a densely connected NN layer (size
10 256, relu activation), followed by a dropout layer (30% during
11 pre-training, 20% during adversarial training) and batch nor-
12 malization. The network core is a Gated Recurrent Unit (GRU,
13 size 256, dropout of 50% during pre-training and 20% during
14 adversarial training). A GRU is a variant of a recurrent network
15 cell with fewer parameters than an LSTM, allowing faster train-
16 ing. The output layer (densely connected NN layer with linear
17 activation) of the generator produces the x, y and z position of
18 21 joints.

19 During pre-training (described in the below Section 5.2), the
20 dropout rate is larger due to the MSE function used in pre-
21 training posing a high probability of overfitting. The MSE gives
22 the generator direct feedback on how far each predicted pose is

from the ground truth. During later multi-adversarial training,
24 the generator receives less direct output feedback and is there-
25 fore less likely to be able to overfit on the dataset. The adver-
26 sarial loss merely tells the generator the likelihood of the dis-
27 criminators(s) finding its output to be real data, without per-pose
numerical error feedback.

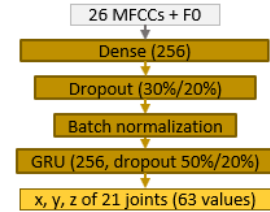


Fig. 8. The generator network. The generator receives 27 prosodic speech features (26 MFCCs + F0) and produces the xyz position of 21 joints. In brackets are denoted the layer size or the dropout ratio; the larger dropout ratios apply to pre-training with MSE.

5.2. Generator pre-training

During later adversarial training (Section 7.1), the generator
will receive feedback based on the phase structure of its motion
output. This phase structure will be determined by the
phase classifier previously described in Section 4. The automatic
phase classification means that no matter what input, a
phase label will be assigned to each time-step. Data points diverging
from a skeleton structure and not resembling human motion
may get assigned an indeterminable phase label. We do
not want very unrealistic data to be assigned a potentially realistic
phase labelling. This could allow for the following scenario:
the generator generates effectively noise, the classifier produces
a realistic phase structure based on this, the generator receives

1 positive feedback for having produced motion with a realistic
 2 phase structure. We therefore first ensure a quality baseline of
 3 generator output that can reasonably be assigned phase labels
 4 by the phase classifier. Hence, before adversarial training, we
 5 initialize the generator to a baseline output resembling a skele-
 6 ton structure.

7 We pre-train the generator with a standard mean squared er-
 8 ror (MSE) loss of generated versus real motion:

$$MSE(m_g, m_r) = \frac{1}{T} \sum_{t=1}^T (m_g - m_r)^2 \quad (1)$$

9 MSE training allows for fast convergence towards a skeleton
 10 structure, but as expected, this training suffers from mean pose
 11 convergence and produces only very damped motions around
 12 the average joint positions. This is visualized in Figure 1f, as
 13 well as in the supplemental video. We use this model as the
 14 starting point for the adversarial training, and utilize the training
 15 history for pre-training the phase discriminator as described in
 16 Section 6.1.

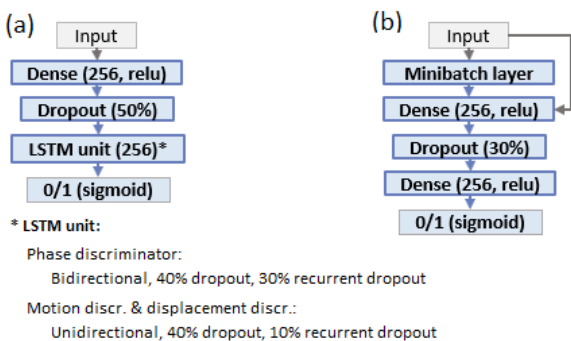


Fig. 9. Network architecture of the adversaries. Left: Phase, motion, and displacement discriminators. Right: Minibatch discriminator. All discriminators apply input transformation via a standard densely connected NN layer. (The minibatch layer applies Equation 2 before the input transformation.) Dropout is applied subsequently, followed by a recurrent unit (left) or another densely connected NN layer (right). The output layer applies a sigmoid activation.

6. Adversaries

18 A training objective with a standard regression loss can be
 19 problematic for gesture generation due to the variability of
 20 speech gesture. The same or a similar utterance may reason-
 21 ably be associated with various different gestures; the generator
 22 may produce a subjectively valid gesture that is nonetheless ob-
 23 jectively far from the ground-truth pose sequence, resulting in a

high training error. A common result is mean pose convergence,
 24 where the generator produces damped motion around the mean,
 25 minimizing error across all possibilities. Our adversarial train-
 26 ing paradigm removes the tight constraint of predicting exact
 27 poses while still enforcing higher-level descriptors of natural
 28 gesture, as well as lower-level humanoid skeleton configuration
 29 constraints.

30 Specifically, in an adversarial training paradigm, the genera-
 31 tor receives as feedback only a single value per generated ges-
 32 ture sequence, representing the decision of the discriminator
 33 whether the presented sequence looks real or not. Therefore,
 34 rather than receiving a numerical error for every pose in a se-
 35 quence as is the case in a standard regression loss, the generator
 36 receives a single, more qualitative judgement about the entire
 37 pose sequence.

38 Our chosen descriptors of natural gesture can be summarized
 39 as three basic objectives: (1) The generator should produce se-
 40 quences of joint positions that represent valid human skeleton
 41 configurations. (2) The produced pose sequences should de-
 42 scribe realistic gesture dynamics, including distinct phases of
 43 e.g. acceleration as well as stillness. (3) The output pose se-
 44 quences should be appropriate with respect to the speech they
 45 accompany. With this selection of objectives, we aim to ensure
 46 that our output can both be considered speech gesture (valid
 47 human skeleton moving according to speech), as well as ad-
 48 dressing the problems in previous works of overly smooth or
 49 lethargic motion, by explicitly enforcing some characteristics
 50 of gesture motion dynamics.

51 In this Section, we will discuss how we represent the above
 52 output objectives with a set of training adversaries, called dis-
 53 criminator, each enforcing a different part of the objectives.
 54 Each discriminator is a separate neural network, with its own
 55 training loss feedback. Their architectures are detailed in Fig-
 56 ure 9; we will describe each discriminator one-by-one below.

6.1. Phase structure discriminator

57 The phase discriminator's job is to determine whether the
 58 generator's output follows a realistic gesture phase structure.
 59 This discriminator therefore only receives phase labels as input

1 rather than joint positions. We additionally provide the phase
 2 discriminator with the pitch value at each time-step as an in-
 3 dicator of speech emphasis. The network architecture of the
 4 phase discriminator is detailed in Figure 9a.

5 Phase labels are always determined by the phase classifier;
 6 that is, we never use the ground truth annotation during adver-
 7 sarial training. This ensures that any differences in the phase
 8 structure of real and generated data is not due to potentially
 9 noisy automatic classification. As the phase labels are auto-
 10 matically determined by the phase classifier, we want to ensure
 11 somewhat sensible input to the classifier, i.e. input resembling
 12 human motion. We utilize the training history of the generator’s
 13 pre-training to prepare the phase discriminator. The training
 14 history of the generator are the generator weights saved peri-
 15 odically during its pre-training described in Section 5.2. The
 16 phase discriminator’s pre-training utilizes this as follows: The
 17 phase discriminator receives the classified phase labelling of
 18 an untrained generator (i.e. noise input). When the phase dis-
 19 criminator achieves an accuracy score of at least 70% for three
 20 batches in a row, the generator gets ‘upgraded’ with the next
 21 set of weights from the training history. This is repeated un-
 22 til the phase discriminator has reached the weights level of the
 23 fully pre-trained generator. This step-by-step upgrading of the
 24 generator’s weights serves to not overwhelm the discriminator
 25 during pre-training.

26 6.2. Motion realism discriminator

27 Adversarial training between the generator and the phase dis-
 28 criminator alone will quickly lead to divergence from the skele-
 29 ton structure due to the phase discriminator only judging the au-
 30 tomatically classified phase labels. As described in Section 5.2,
 31 the phase classifier may assign a realistic phase structure to un-
 32 realistic input; when the generator is judged solely on this phase
 33 structure, it may receive positive discriminator feedback for en-
 34 tirely unrealistic output and we found this to lead to increasing
 35 divergence from skeleton-like joint positions. To address
 36 this problem, we employ a second discriminator that judges the
 37 output of the generator directly by receiving the raw generated
 38 joint positions, as well as the corresponding audio features. The

63 joint values (x, y, z of 21 joints) and 27 speech features are
 39 passed into the network architecture detailed in Figure 9a.

40 The motion realism discriminator is pre-trained in a classic
 41 adversarial training setting with a new generator in order to
 42 learn to detect unrealistic point clouds not resembling a skele-
 43 ton. This is necessary in order to not allow the already pre-
 44 trained generator to regress to non-humanoid point clouds.

45 6.3. Minibatch discriminator

46 Adversarial training is prone to suffering from mode col-
 47 lapsed, where the generator produces repetitive patterns of out-
 48 put. While the discriminator can immediately learn that this
 49 specific pattern comes from the generator, the generator only
 50 needs to shift its repetitive output slightly to fool the discrimi-
 51 nator. This may be repeated in an infinite cat and mouse game.
 52 One reason for this mode collapse is that a standard discrimi-
 53 nator only judges one output sequence at a time, rather than
 54 in the context of a whole batch of data. A minibatch layer can
 55 be added to allow the discriminator to see this context and en-
 56 sure that the generator cannot get away with even novel patterns
 57 when they are repetitive throughout the data batch [49].

58 Instead of integrating minibatch discrimination into the motion
 59 realism discriminator, we achieved better performance
 60 when outsourcing the task to a separate discriminator. This dis-
 61 criminator receives 63 joint values (x,y,z of 21 joints) generated
 62 by the generator or taken from the ground truth and calculates
 63 a minibatch similarity measure:

$$sim(X) = L^1(W \cdot X), \quad (2)$$

64 where L^1 denotes the L1 norm and W is a 300-dimensional
 65 (trainable) weight tensor. The detailed architecture of the mini-
 66 batch discriminator is shown in Figure 9b.

67 6.4. Displacement discriminator

68 The generator’s output at the beginning of adversarial train-
 69 ing is the damped motion learned from the MSE pre-training.
 70 To encourage the generator towards less damped motion, we
 71 introduce a displacement discriminator that receives the same
 72 motion input as the phase classifier, namely the per-frame x,
 73 y, and z offset of the 16 arm joints (48 values). That is, the

1 displacement discriminator explicitly sees how much each joint
 2 has moved at each time-step; it can penalize a generator that
 3 produces very slow (or very fast) motion. In effect, the dis-
 4 placement discriminator judges the directional velocity of the
 5 generated joint positions. The displacement discriminator also
 6 serves to reduce jitter in the motion (offset in one direction al-
 7 ways followed by some offset to opposite direction).

8 The error from this discriminator receives a lesser weight and
 9 serves as a minor side objective of the generator training, help-
 10 ing to stabilize and speed up convergence and smooth output
 11 motion. The architecture of the displacement discriminator fol-
 12 lows that of the motion realism discriminator and is visualized
 13 in Figure 9a.

14 7. Training process

15 During adversarial training, the generator’s output is judged
 16 by all discriminators and an averaged error is computed, as de-
 17 tailed in Section 7.1 below. This is followed by a training step of
 18 objective numerical errors. The objective error functions speed
 19 up convergence and enable continuous prediction, as described
 20 in Section 7.2.

21 7.1. Adversarial training

22 The adversarial training is visualized in Figure 10 and sum-
 23 marized below:

- 24 • The **generator** receives 27 prosodic speech features as in-
 25 put and generates corresponding 3D positions of 21 joints.
- 26 • The **phase classifier** first converts the joint positions to
 27 frame offsets and subsequently predicts a sequence of ges-
 28 ture phase labels. The phase classifier also receives as in-
 29 put the F0 (pitch) value of each frame. The classifier’s
 30 weights are fixed during adversarial training.
- 31 • The produced phase label sequence of the classifier, plus
 32 the F0 value, serve as input for the **phase structure dis-**
 33 **cri****minator**.
- 34 • The **motion realism discriminator** receives the joint po-
 35 sitions directly, as well as all corresponding 27 speech fea-
 36 tures.

- The **displacement discriminator** receives the same mo-
 37 tion input as the phase classifier, the per-frame joint offsets
 38 of the 16 arm and hand joints.
- The **minibatch discriminator** only receives the joint po-
 40 sitions as input.

42 All three discriminators are trained with a binary cross-entropy
 43 loss to determine whether a motion sequence is real or gener-
 44 ated. The discriminators learn independently from each other,
 45 sharing no weights and receiving individual training loss feed-
 46 back. The loss of the generator with respect to the three dis-
 47 criminator is weighted and combined into a single value for
 48 the generator’s training step. All models work with input se-
 49 quences of 5 seconds, at 20 fps, resulting in 100 time-steps.

50 During adversarial training steps, the generator optimizes the
 51 binary cross-entropy of the discriminators’ output. The gener-
 52 ator’s training error with respect to the four discriminators is
 53 averaged for each optimization step in the following manner:

$$54 \mathcal{L}_{GAN}(G) = \\ 55 \frac{w_p \mathcal{L}(G, D_p) + w_r \mathcal{L}(G, D_r) + w_m \mathcal{L}(G, D_m) + w_d \mathcal{L}(G, D_d)}{w_p + w_r + w_m + w_d}, \quad (3)$$

56 with $w_p = 2$, $w_r = 4$, $w_m = 4$, and $w_d = 1$,

57 where w_p is the weight assigned to the phase discriminator’s
 58 loss, w_r the weight for the motion realism discriminator, w_m the
 59 weight for the minibatch discriminator, and w_d the weight for
 60 the displacement discriminator. $\mathcal{L}(G, D)$ represents the genera-
 61 tor’s objective with respect to one discriminator. The weighting
 62 of 2:4:4:1 was chosen by empirically finding values that led
 63 to stable training with respect to all discriminator objectives,
 64 without the generator collapsing with respect to one or more
 65 objectives. The adversarial training of the generator is visual-
 66 ized in Figure 10, representing a more detailed version of the
 67 previously presented Figure 5. We use the RMSprop optimizer
 68 during adversarial training.

69 7.2. Objective loss penalties

70 In addition to the adversarial updates of the generator, one
 71 MSE correction is performed per two adversarial steps. The

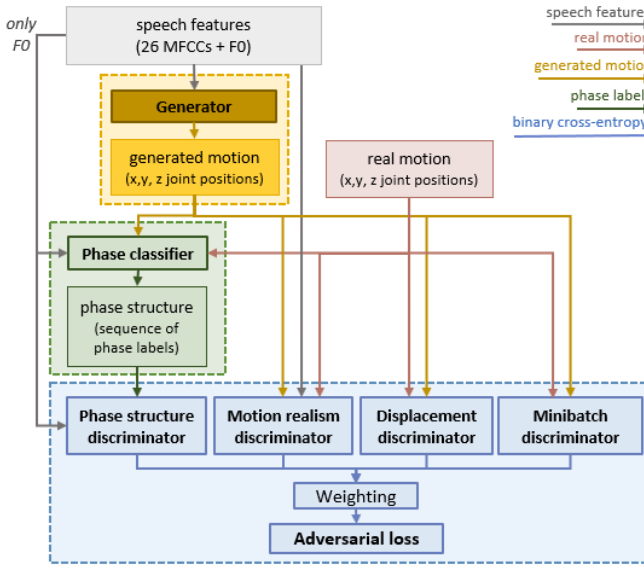


Fig. 10. Adversarial training. The generator produces joint positions based on input speech features. Its output is judged by four discriminators with separate objectives, and a weighted error is computed with respect to all four evaluations. Each discriminator optimizes the binary cross-entropy objective, deciding if a given data sample is real or generated.

MSE avoids major deviations of the generator's output from a realistic skeleton structure that would produce nonsensical phase label output and slow down the training overall. An alternative, similar approach would be to restrict joint positions to realistic ranges.

The generator is trained to predict gesture motion for 5 seconds of speech input at a time rather than for continuous input. Gesture motion is therefore continuous within 5 second prediction intervals, but can be visibly discontinuous between intervals. To avoid having to compute smooth transitions in post-processing, we introduce a penalty for the generator for discontinuous sequences within a training batch. The discontinuation penalty is computed as the mean squared distance between the start position of a sequence and the end position of the preceding sequence. The penalty for first sequence within a batch is always set to zero and otherwise:

$$\mathcal{L}_{cont}(G) = \frac{1}{T} \sum_{t=1}^T (G(x)(t) - G(x)(t-1))^2. \quad (4)$$

We observed during adversarial training that the predicted finger positions often move far from the hand. To speed up the training process, we added a simple finger distance penalty restricting the predictions to realistic ranges. We compute the

distance of each finger marker to the respective hand marker and calculate the MSE with respect to the real distances:

$$\mathcal{L}_{fingers}(G) = \frac{1}{n} \sum_{i=1}^n (\mathcal{D}_{fingers}(G(x)) - \mathcal{D}_{fingers}(Y(x)))^2 \quad (5)$$

with $Y(x)$ denoting the ground truth for sample x , and $\mathcal{D}_{fingers}$ computed as the concatenation of each finger marker's x, y, and z distance from the respective hand.

8. Results

We conducted a series of qualitative evaluations to clarify the roles of each discriminator and their benefits for generator training, and quantitative evaluations of the resulting generator output.

8.1. Qualitative evaluation

In this section, we discuss how each discriminator as well as the objective loss penalties affects the output of the generator qualitatively.

8.1.1. Phase structure discriminator

The phase structure discriminator allows us to capture important gesture dynamics without having to rely on implicit learning from a larger dataset (such as in Ginosar et al. [33]). During the pre-training described in Section 6.1, this discriminator easily learns to distinguish the (noisy) classified phase structures of real motion and motion produced by the pre-trained generator. During adversarial training, the phase discriminator's accuracy remains balanced with the generator's while the generator's output is improving in quality. We visualize the benefits of the phase discriminator for encouraging better gesture motion dynamics in the supplemental video; without the phase discriminator, the motion shows no clear holds or accelerations characteristic of the stroke phase. The motion appears to correspond less with the speech prosody.

8.1.2. Motion realism discriminator

The phase discriminator's judgment alone is not a sufficient constraint for the generator's output. As described in Section 6.2, the automatic phase label classification of the generator's

1 output and the phase classifier’s naivety with respect to non-
 2 human point clouds provides too much room for the generator
 3 to produce unrealistic data. The motion discriminator presents
 4 a better constraint for maintaining a skeleton structure as it sees
 5 the generator’s output directly and successfully constrains the
 6 generator to data points resembling a skeleton structure. Fig-
 7 ure 1e visualizes the output distribution produced by a genera-
 8 tor unconstrained by a motion discriminator. The supplemen-
 9 tal video also shows a sample of the motion produced without
 10 a motion realism discriminator; the joint positions move away
 11 from the skeleton structure, producing output not resembling
 12 human motion.

13 8.1.3. Minibatch discriminator

14 As a vanilla discriminator only judges output sequences in
 15 isolation, without taking the context of the data batch into con-
 16 sideration, the generator can suffer from mode collapse, as de-
 17 scribed in 6.3, and visualized by the plotted data distribution in
 18 Figure 1c. Our minibatch discriminator successfully forces the
 19 generator to produce more diverse output. The supplemental
 20 video shows the repetitive motion generated under mode col-
 21 lapsed, as well as the improved, more diverse output with mini-
 22 batch discrimination. We considered two alternative integra-
 23 tions of minibatch discrimination into our model, namely as
 24 part of the motion realism discriminator and as part of a separate
 25 discriminator. In practice, we find the adversarial training to be
 26 more stable when outsourcing the minibatch discrimination to a
 27 separate discriminator only receiving motion input. Generator
 28 training was less likely to collapse with respect to one discrimi-
 29 nator when the adversarial objective was more distributed. The
 30 benefit of employing multiple discriminators has also been dis-
 31 cussed in previous works [50, 51].

32 8.1.4. Displacement discriminator

33 Learning from the phase discriminator’s feedback is poten-
 34 tially difficult for the generator due to the hidden layers between
 35 the generator and phase discriminator (i.e., the phase classifier’s
 36 computations that are inaccessible to the generator). The gen-
 37 erator’s motion output is first converted to per-frame offsets of
 38 the joints and then passed to the classifier for higher level fea-

ture extraction. Introducing a discriminator receiving the same
 39 processed motion as the classifier can provide more direct feed-
 40 back. In practice, we found that the addition of such a dis-
 41 placement discriminator sped up learning and moved predic-
 42 tions away faster from the damped baseline motion produced by
 43 the pre-trained generator. We visualize this by plotting an ex-
 44 ample data distribution in Figure 1d. The slow departure from
 45 the mean pose when training the model without the displace-
 46 ment discriminator is also shown in the supplemental video. We
 47 also illustrate the smoothing benefit of the displacement dis-
 48 criminator in the video: When training the generator without
 49 any discriminator receiving the joint offsets (i.e. with neither
 50 the displacement discriminator nor the phase classifier and dis-
 51 criminator), the motion output displays a great amount of jitter.
 52 We show that adding the displacement discriminator reduces
 53 jitter to a large degree. This discriminator receives the smallest
 54 weighting in the generator’s objective.

55 8.1.5. Adversarial error weighting

56 We find a weighting of 2:4:4:1 for the error of the phase dis-
 57 criminator, motion realism discriminator, minibatch discrim-
 58 inator, and the displacement discriminator, respectively, to
 59 achieve the most stable training, measured by the accuracy of
 60 the binary cross-entropy objective for each discriminator. This
 61 weighting allows us to see stable accuracy improvements for
 62 the generator across all adversarial objectives without collapse
 63 with regard to one or more objectives.

64 8.1.6. Objective losses

65 The discontinuation penalty is largely successful in reduc-
 66 ing the positional jumps between predicted motion sequences,
 67 making the model more applicable for continuous gesture gen-
 68 eration for long sequences of speech input. The finger distance
 69 penalty proved a simple measure to avoid unrealistic finger po-
 70 sitions without strongly constraining the generator in its predic-
 71 tions.

72 8.2. Quantitative evaluation

73 We provide a quantitative evaluation of our generation results
 74 based on the wrist motion in Figure 11. We present these results

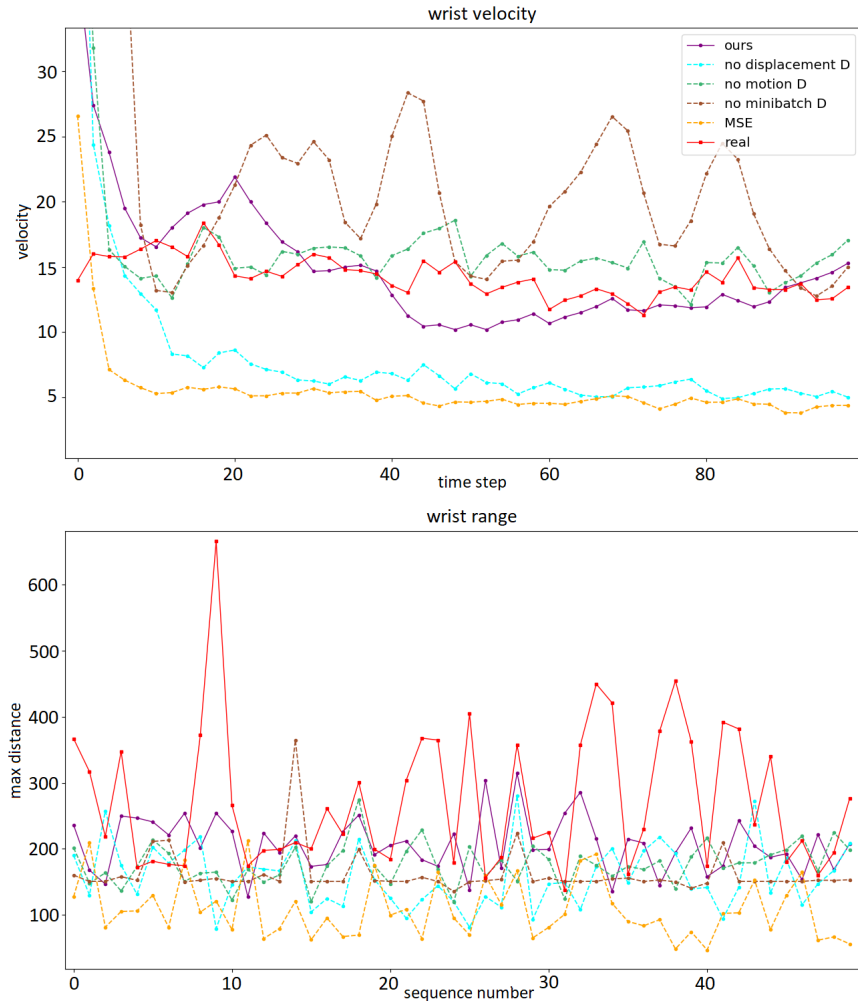


Fig. 11. Quantitative gesture generation evaluation. Top: Wrist velocity for each predicted time step, median across 150 sequences (see Equations 6 and 7). **Bottom:** Maximum distance of the wrists from mean pose for 50 randomly selected sequences.

in an ablation manner, as in Figure 1, evaluating how removal of a specific discriminator in training affects the generation result.

The top graph plots the wrist velocity per predicted time step, each representing the median over 150 predicted gesture sequences. This 1-dimensional velocity of the 3-dimensional x, y, z joint coordinates of a time step t and a sequence i is more specifically calculated as follows:

$$velocity(t^i) = |x_{t^i} - x_{t^{i-1}}| + |y_{t^i} - y_{t^{i-1}}| + |z_{t^i} - z_{t^{i-1}}| \quad (6)$$

$$velocity(t) = median(t^0, t^1, \dots, t^n) \quad (7)$$

We can see that one of the closest matches of real motion (red) are achieved by our model (purple) and the system configuration removing the motion discriminator (green). However, the latter configuration generates joint positions that heavily vi-

olate human skeleton constraints. Removing the minibatch discriminator (brown) produces faster than real motion, as well as resulting in highly repetitive output. The output under removal of the displacement discriminator (blue) as well as the output the generator trained solely with a mean squared error loss (yellow) exhibits very slow motion, much below realistic levels.

The bottom graph in Figure 11 plots the maximum distance travelled away from the mean pose, for 50 example sequences. The closest match to real wrist position ranges is achieved by our model, though it does not reach the wide ranges of real motion. The MSE-trained generator and the no-displacement-discriminator condition show a comparable level of variation to real motion, but the gestures are overall closer to the body

1 both than real motion and than for our model. The no-motion-
 2 discriminator condition similarly produces lower ranges than
 3 real motion. The no-minibatch-discriminator condition pro-
 4 duces very stable ranges, indicative of the repetitive gesture se-
 5 quences generated.

6 9. Discussion

7 We explored generative adversarial networks for speech-to-
 8 gesture translation with higher level feature extraction. For this
 9 purpose, we first recorded a dataset of over six hours of nat-
 10 ural, conversational speech with high-quality 3D motion cap-
 11 ture. Gesture motion is marked by distinct dynamics, including
 12 phases of acceleration and effort, of pause, and of relaxation.
 13 These higher-level dynamics can be difficult to capture implic-
 14 itly. To enforce these dynamics more explicitly in a top-down
 15 manner, we train a classifier to detect gesture phases automati-
 16 cally, and then train a phase structure discriminator to detect
 17 realistic versus non-realistic phase sequences.

18 To train the phase classifier, we hand-annotated the phases
 19 of an over 3.7 hour long subset of our dataset using 9 differ-
 20 ent phase labels. We validate our results on a second speaker,
 21 for whom we annotate an additional small sample of gesture
 22 sequences. We compare three models of phase classification
 23 with different levels of detail (1-, 4-, and 6-class classification).
 24 We achieve good results, and we conclude that our error rate
 25 may to a relatively large extend be due to inter-coder incon-
 26 sistencies. This leads to the dilemma of weighing data quan-
 27 tity against data quality; the large time requirement of hand-
 28 annotation (1 hour or more work for 1 minute of data) tempts
 29 distributing the work load across a number of people, but this
 30 may lead to increased problems with annotation consistency.
 31 When motion capture is available, we suggest that automati-
 32 cally pre-annotating all sections with close to zero velocity as
 33 ‘hold’ could speed up the annotation process as well as increase
 34 inter-coder agreement in future work.

35 Our 1-class stroke classifier performs similarly well on both
 36 our speaker and the validation speaker. 4- and 6-class classi-
 37 fication reaches equal scores for our speaker; for the valida-
 38 tion speaker, the 4-class model achieves a significantly higher

39 score. One reason for the drop in performance on the valida-
 40 tion speaker for the multi-phase models may be differences in
 41 speaker style, leading to different expressions of gesture phase.
 42 The higher the level of detail, the larger are the expected inter-
 43 speaker differences. Ideal phase classification may therefore
 44 always be speaker-specific.

45 For training our gesture generator, instead of using a stan-
 46 dard regression loss, we construct a generative adversarial set-
 47 ting with multiple discriminators. We observe a clear advantage
 48 of adversarial training over using a standard regression loss; the
 49 produced motion has a larger positional range, more realistic
 50 velocity, and appears much less damped.

51 By using multiple discriminators, we can phrase the speech-
 52 to-gesture generation problem as a series of sub-problems. We
 53 use our automatic phase labelling to enforce a more realistic
 54 gesture phase structure in our output; this is the task of the phase
 55 structure discriminator. The phase structure discriminator en-
 56 ables the enforcement of higher level dynamic characteristics
 57 in the output without having to rely on implicit learning from a
 58 large amount of data.

59 Because an automatic phase classifier will always assign
 60 some phase label to even random point clouds, we constrain the
 61 motion output with a second discriminator judging the gener-
 62 ated joint positions as real or fake; this is the task of the motion
 63 realism discriminator. Because the motion realism discrimina-
 64 tor’s task is to judge one generated motion sequence at a time, it
 65 can allow for the same sequence to be generated repeatedly. A
 66 minibatch discriminator detects such repetitive patterns, ensur-
 67 ing diversity in the output. Lastly, generated motion can often
 68 look jittery; we address this by including a the training objec-
 69 tive of realistic joint displacement per frame, monitored by the
 70 displacement discriminator.

71 To our knowledge, this is the first work using adversarial
 72 training for generating 3D gesture motion from natural speech,
 73 and the first work exploring the use of multiple discriminators
 74 for the purpose. We observe a benefit of using multiple dis-
 75 criminator to stabilize adversarial training, and we report how
 76 each discriminator addresses a distinct sub-problem in the ges-

ture generation task. We employ explicit modelling of the dynamics of gesture motion to allow learning of these higher level features from a smaller dataset. We see our work as a further step towards enabling automatic animation of realistic conversational agents.

Our results are limited to gesture generation for the single speaker we recorded and more data of various speakers would be necessary to make generalizations. Due to the high variance of gesture behavior across speakers, this is a very difficult task. Because we generate gesture motion from prosodic speech features, semantically meaningful gestures can hardly be inferred without explicitly employing speech recognition methods. Speech recognition, however, would likely only yield a benefit when using a much larger dataset, ensuring a number of examples of the same phrases.

10. Future work

While generated motion improved greatly with respect to standard regression loss training, the produced motion still lacks desirable levels of realism. Looking forward, we will explore other measures of realism that may complement adversarial training.

We are interested in working towards explicit enforcement of gesture phase by using the gesture phase as a conditional input for the generator, comparable to the approach proposed by Holden et al. [29], who use locomotion phase as input in a character control system. This may require gesture phase extraction solely from input speech, rather than motion data. In this regard, Yunus et al. [48] report interesting initial results in predicting gesture phase from prosodic speech features.

Using our gesture phase extraction, we want to analyze speech gesture further to understand better the relationship of gesture characteristic and accompanying speech. Considering the suggested differences in phase expression, as well previously found differences in gesture style (e.g. Ginosar et al. [33]), we want to investigate how gesture meaning can, or cannot, be compared across speakers.

We are also looking to explore the use of convolutional networks within a generative adversarial paradigm, such as in Gi-

nosar et al. [33], exploring visual data representations of speech as well as motion.

Acknowledgments

This research was funded by Science Foundation Ireland under the ADAPT Centre for Digital Content Technology (Grant 13/RC/2016). Partial funding was also provided through NSF grant 1748058.

References

- [1] Kang, SH, Feng, AW, Seymour, M, Shapiro, A. Smart mobile virtual characters: Video characters vs. animated characters. In: Proceedings of the Fourth International Conference on Human Agent Interaction. ACM; 2016, p. 371–374.
- [2] Salem, M, Rohlfing, K, Kopp, S, Joublin, F. A friendly gesture: Investigating the effect of multimodal robot behavior in human-robot interaction. Proceedings - IEEE International Workshop on Robot and Human Interactive Communication 2011;:247–252doi:10.1109/ROMAN.2011.6005285.
- [3] McNeill, D. Hand and mind: What gestures reveal about thought. University of Chicago press; 1992.
- [4] Melinger, A, Levelt, WJ. Gesture and the communicative intention of the speaker. Gesture 2004;4(2):119–141.
- [5] De Ruiter, JP, Bangerter, A, Dings, P. The interplay between gesture and speech in the production of referring expressions: Investigating the tradeoff hypothesis. Topics in Cognitive Science 2012;4(2):232–248.
- [6] Ferstl, Y, Neff, M, McDonnell, R. Multi-objective adversarial gesture generation. In: Motion, Interaction and Games. 2019, p. 1–10.
- [7] Cassell, J, Vilhjálmsson, HH, Bickmore, T. BEAT: the Behavior Expression Animation Toolkit. ACM Transactions on Graphics 2001;:477–486URL: <http://dl.acm.org/citation.cfm?id=383315>. doi:10.1007/978-3-662-08373-4_8.
- [8] Thiebaut, M, Marsella, S, Marshall, AN, Kallmann, M. SmartBody: behavior realization for embodied conversational agents. In: Proceedings of International Joint Conference on Autonomous Agents and Multiagent Systems. Aamas. ISBN 978-0-9817381-0-9 LK; 2008, p. 151–158. URL: <http://dl.acm.org/citation.cfm?id=1402409>. doi:10.1016/j.ais.2009.01.020.
- [9] Marsella, S, Xu, Y, Lhommet, M, Feng, A, Scherer, S, Shapiro, A. Virtual character performance from speech. In: Proceedings of the 12th ACM SIGGRAPH/Eurographics Symposium on Computer Animation. ISBN 9781450321327; 2013, p. 25–35. URL: <http://dl.acm.org/citation.cfm?doid=2485895.2485900>. doi:10.1145/2485895.2485900.
- [10] Neff, M, Kipp, M, Albrecht, I, Seidel, HP. Gesture modeling and animation based on a probabilistic re-creation of speaker style. ACM Transactions on Graphics 2008;27(1):1–24. URL: <http://portal.acm.org/citation.cfm?doid=1330511.1330516>. doi:10.1145/1330511.1330516.
- [11] Bergmann, K, Kopp, S. GNetIc - Using bayesian decision networks for iconic gesture generation. Lecture Notes in Computer Science (including subseries Lecture Notes in Artificial Intelligence and Lecture Notes in Bioinformatics) 2009;5773 LNAI:76–89. doi:10.1007/978-3-642-04380-2_12.
- [12] Bergmann, K, Kopp, S. Increasing the expressiveness of virtual agents: autonomous generation of speech and gesture for spatial description tasks. Proceedings of The 8th International Conference on Autonomous Agents and Multiagent Systems-Volume 1 2009;:361–368URL: <http://portal.acm.org/citation.cfm?id=1558013.1558062>.
- [13] Kallmann, M, Marsella, S. Hierarchical motion controllers for real-time autonomous virtual humans. In: International Workshop on Intelligent Virtual Agents. Springer; 2005, p. 253–265.

[14] Thiebaux, M, Marsella, S, Marshall, AN, Kallmann, M. Smartbody: Behavior realization for embodied conversational agents. In: Proceedings of the 7th international joint conference on Autonomous agents and multiagent systems-Volume 1. International Foundation for Autonomous Agents and Multiagent Systems; 2008, p. 151–158.

[15] Neff, M. Hand gesture synthesis for conversational characters. *Handbook of Human Motion* 2016;1:1–12.

[16] Levine, S, Theobalt, C, Koltun, V. Real-time prosody-driven synthesis of body language. *ACM Transactions on Graphics* 2009;28(5):1. doi:10.1145/1618452.1618518.

[17] Levine, S, Krähenbühl, P, Thrun, S, Koltun, V. Gesture controllers. *ACM Transactions on Graphics* 2010;29(4). URL: <http://dl.acm.org/citation.cfm?id=1778861>. doi:10.1145/1833351.1778861.

[18] Chiu, CC, Marsella, S. Gesture Generation with Low-Dimensional Embeddings. In: Proceedings of the 2014 international conference on Autonomous agents and multi-agent systems. 2014, p. 781–788.

[19] Chiu, CC, Marsella, S. How to train your avatar: A data driven approach to gesture generation. *Lecture Notes in Computer Science (including subseries Lecture Notes in Artificial Intelligence and Lecture Notes in Bioinformatics)* 2011;6895 LNAI:127–140. doi:10.1007/978-3-642-23974-8_14.

[20] Bozkurt, E, Yemez, Y, Erzin, E. Multimodal analysis of speech and arm motion for prosody-driven synthesis of beat gestures. *Speech Communication* 2016;85:29–42. URL: <http://dx.doi.org/10.1016/j.specom.2016.10.004>. doi:10.1016/j.specom.2016.10.004.

[21] Chiu, CC, Marsella, S. Predicting Co-verbal Gestures: A Deep and Temporal Modeling Approach. *International Conference on Intelligent Virtual Agents* 2015;9238 of th(August 2015):152–166. URL: http://link.springer.com/chapter/10.1007/978-3-319-21996-7_17. doi:10.1007/978-3-319-21996-7_17.

[22] Ferstl, Y, McDonnell, R. Investigating the use of recurrent motion modelling for speech gesture generation. In: *IVA '18: International Conference on Intelligent Virtual Agents (IVA '18)*. 2018, p. 93–98.

[23] Hasegawa, D. Evaluation of Speech-to-Gesture Generation Using Bi-Directional LSTM Evaluation of Speech-to-Gesture Generation Using Bi-Directional LSTM Network. In: *IVA '18: International Conference on Intelligent Virtual Agents (IVA '18)*. November. ISBN 9781450360135; 2018, doi:10.1145/3267851.3267878.

[24] Kucherenko, T, Hasegawa, D, Henter, GE, Kaneko, N, Kjellström, H. Analyzing input and output representations for speech-driven gesture generation. In: *IVA '19: International Conference on Intelligent Virtual Agents (IVA '19)*. 2019.

[25] Pavlo, D, Grangier, D, Auli, M. Quaternet: A quaternion-based recurrent model for human motion. *arXiv preprint arXiv:180506485* 2018;.

[26] Li, Z, Zhou, Y, Xiao, S, He, C, Li, H. Auto-conditioned lstm network for extended complex human motion synthesis. *arXiv preprint arXiv:170705363* 2017;3.

[27] Martinez, J, Black, MJ, Romero, J. On human motion prediction using recurrent neural networks 2017;URL: <http://arxiv.org/abs/1705.02445>. doi:10.1109/CVPR.2017.497. arXiv:1705.02445.

[28] Jain, A, Zamir, AR, Savarese, S, Saxena, A. Structural-RNN: Deep Learning on Spatio-Temporal Graphs 2015;;5308–5317URL: <http://arxiv.org/abs/1511.05298>. doi:10.1109/CVPR.2016.573. arXiv:1511.05298.

[29] Holden, D, Komura, T, Saito, J. Phase-functioned neural networks for character control. *ACM Transactions on Graphics (TOG)* 2017;36(4):42.

[30] Barsoum, E, Kender, J, Liu, Z. Hp-gan: Probabilistic 3d human motion prediction via gan. In: *Proceedings of the IEEE Conference on Computer Vision and Pattern Recognition Workshops*. 2018, p. 1418–1427.

[31] Kundu, JN, Gor, M, Babu, RV. Bihmp-gan: Bidirectional 3d human motion prediction gan. *arXiv preprint arXiv:181202591* 2018;.

[32] Sadoughi, N, Busso, C. Novel realizations of speech-driven head movements with generative adversarial networks. In: *2018 IEEE International Conference on Acoustics, Speech and Signal Processing (ICASSP)*. IEEE; 2018, p. 6169–6173.

[33] Ginosar, S, Bar, A, Kohavi, G, Chan, C, Owens, A, Malik, J. Learning individual styles of conversational gesture. In: *Proceedings of the IEEE Conference on Computer Vision and Pattern Recognition*. 2019, p. 3497–3506.

[34] Ronneberger, O, Fischer, P, Brox, T. U-net: Convolutional networks for biomedical image segmentation. In: *International Conference on Medical image computing and computer-assisted intervention*. Springer; 2015, p. 234–241.

[35] Kendon, A. Some relationships between body motion and speech. *Studies in dyadic communication* 1972;7(177):90.

[36] Kita, S, Gijn, IV, Hulst, HVD. Movement Phases in Signs and Co-speech Gestures, and Their Transcription by Human Coders. *Gesture and sign language in human-computer interaction : international gesture workshop Bielefeld* 1997;:23–35.

[37] Kita, S. The temporal relationship between gesture and speech: A study of japanese-english bilinguals. *MS, Department of Psychology, University of Chicago* 1990;90:91–94.

[38] Madeo, RCB, Peres, SM, Lima, CADM. Gesture phase segmentation using support vector machines. *Expert Systems with Applications* 2016;56:100–115. URL: <http://dx.doi.org/10.1016/j.eswa.2016.02.021>. doi:10.1016/j.eswa.2016.02.021.

[39] Martell, C, Kroll, J. Corpus-based gesture analysis: an extension of the form dataset for the automatic detection of phases in a gesture. *International Journal of Semantic Computing* 2007;1(04):521–536.

[40] Alexanderson, S, House, D, Beskow, J. Automatic annotation of gestural units in spontaneous face-to-face interaction. *Proceedings of the Workshop on Multimodal Analyses enabling Artificial Agents in Human-Machine Interaction - MA3HMI '16* 2016;:15–19URL: <http://dl.acm.org/citation.cfm?doid=3011263.3011268>. doi:10.1145/3011263.3011268.

[41] Gebre, BG, Wittenburg, P, Lenkiewicz, P. Towards automatic gesture stroke detection. In: *LREC 2012: 8th International Conference on Language Resources and Evaluation*. European Language Resources Association; 2012, p. 231–235.

[42] Bryll, R, Quek, F, Esposito, A. Automatic hand hold detection in natural conversation. In: *IEEE Workshop on Cues in Communication*. 2001, p. 1–4.

[43] Kipp, M, Neff, M, Kipp, KH, Albrecht, I. Towards Natural Gesture Synthesis : Evaluating gesture units in a data-driven approach to gesture synthesis. *Synthesis* 2007;;1–14URL: http://dx.doi.org/10.1007/978-3-540-74997-4_2. doi:10.1007/978-3-540-74997-4_2.

[44] Eyben, F, Weninger, F, Gross, F, Schuller, B. Recent developments in opensmile, the munich open-source multimedia feature extractor. In: *Proceedings of the 21st ACM international conference on Multimedia*. ACM; 2013, p. 835–838.

[45] Kipp, M. Anvil-a generic annotation tool for multimodal dialogue. In: *Seventh European Conference on Speech Communication and Technology*. 2001,.

[46] Artstein, R, Poesio, M. Inter-coder agreement for computational linguistics. *Computational Linguistics* 2008;34(4):555–596.

[47] Valbonesi, L, Ansari, R, McNeill, D, Quek, F, Duncan, S, McCullough, KE, et al. Multimodal signal analysis of prosody and hand motion: Temporal correlation of speech and gestures. In: *2002 11th European Signal Processing Conference*. IEEE; 2002, p. 1–4.

[48] Yunus, F, Clavel, C, Pelachaud, C. Gesture class prediction by recurrent neural network and attention mechanism. In: *Proceedings of the 19th ACM International Conference on Intelligent Virtual Agents*. ACM; 2019, p. 233–235.

[49] Salimans, T, Goodfellow, I, Zaremba, W, Cheung, V, Radford, A, Chen, X. Improved techniques for training gans. In: *Advances in neural information processing systems*. 2016, p. 2234–2242.

[50] Durugkar, I, Gemp, I, Mahadevan, S. Generative multi-adversarial networks. *arXiv preprint arXiv:161101673* 2016;.

[51] Albuquerque, I, Monteiro, J, Doan, T, Considine, B, Falk, T, Mitliagkas, I. Multi-objective training of generative adversarial networks with multiple discriminators. *arXiv preprint arXiv:190108680* 2019;.